Biosensors and Bioelectronics 243 (2024) 115790

Contents lists available at ScienceDirect

Biosensors and Bioelectronics

journal homepage: www.elsevier.com/locate/bios

New insights into the on-site monitoring of probiotics eDNA using biosensing technology for heat-stress relieving in coral reefs

Liwei Wang [a,b,c,d,1], Qi Bin [a,1], Hongjie Liu [a], Yibo Zhang [a], Shaopeng Wang [a], Songlin Luo [a], Zhenghua Chen [a,b], Man Zhang [a,b,**], Kefu Yu [a,b,d,*]

[a] School of Marine Sciences, School of Resources, Environment and Materials, School of Chemistry and Chemical Engineering, Guangxi University, Nanning, 530004, China
[b] Coral Reef Research Center of China, Guangxi Laboratory on the Study of Coral Reefs in the South China Sea, Nanning, 530004, China
[c] Guangxi, Key Laboratory of Processing for Non-ferrous Metallic and Featured Materials, Nanning, 530004, China
[d] Southern Marine Science and Engineering Guangdong Laboratory (Guangzhou), Guangzhou, 511458, China

ARTICLE INFO

Keywords:
Electrochemical biosensor
On-site detection
Coral probiotic
Cobetia marina
eDNA

ABSTRACT

Coral probiotics can improve the tolerance of corals to heat stress, thus mitigating the process of coral thermal bleaching. Sensitive and specific detection of coral probiotics at low abundances is highly desirable but remains challenging, especially for rapid and on-site detection of coral probiotics. Since the electrochemical biosensor has been recently used in the field of environmental DNA (eDNA) detection, herein, an efficient electrochemical biosensor was developed based on $CoS_2/CoSe_2$-NC HNCs electrode material with a specific DNA probe for the *C. marina* detection. After optimization, the lower limit of detection (LOD) values of such biosensors for the target DNA and genomic DNA were 1.58 fM and 6.5 pM, respectively. On this basis, a portable device was constructed for the practical detection of *C. marina* eDNA, and its reliability and accuracy were verified by comparison with the ddPCR method ($P > 0.05$). For each analysis, the average cost was only ~ $1.08 and could be completed within 100 min with reliable sensitivity and specificity. Overall, the biosensor could reflect the protective effect of probiotics on coral heat stress, and the proposed technique will put new insights into the rapid and on-site detection of coral probiotics to assist corals against global warming.

1. Introduction

Global coral coverage has deteriorated over the past two to three decades due to intensifying marine heat waves (Buerger et al., 2020; Quigley et al., 2022). Coral probiotics have been used to improve corals' tolerance and resilience to environmental stress, which is regarded as one of the effective means to mitigate coral bleaching (Maire and van Oppen, 2022; Thatcher et al., 2022). The prospective study (Rosado et al., 2019) has shown that the coral probiotic *Cobetia marina* can release large amounts of catalase (CAT) at 30 °C, which can break down reactive oxygen species (ROS) that cause coral bleaching. The abundance of colonized probiotics is positively correlated with the ability of corals to tolerate environmental stress (Silva et al., 2021). Currently, the main methods used to detect coral probiotics are fluorescence quantitative PCR (qPCR) (Liu et al., 2020) and droplet digital PCR (ddPCR) (Ushijima et al., 2023). However, the main shortcomings, such as the collection of endangered corals (Tandon et al., 2020) as well as tedious sample pre-treatment (Liu et al., 2019; Xia et al., 2022), hinder the implementation of the task of convenient and on-site detection of coral probiotics. In contrast, environmental DNA (eDNA) technology is ideal for coral probiotic monitoring, since it allows direct analysis of eDNA extracted from a large number of environmental samples (e.g., soil, air, or water) without the need to isolate and cultivate any of the target organisms (Huang et al., 2022; Mauvisseau et al., 2022).

Recently, eDNA technology has been identified as a handy, efficient, and non-invasive alternative monitoring method extensively applied in

* Corresponding author. School of Marine Sciences, School of Resources, Environment and Materials, School of Chemistry and Chemical Engineering, Guangxi University, Nanning, 530004, China.
** Corresponding author. School of Marine Sciences, School of Resources, Environment and Materials, School of Chemistry and Chemical Engineering, Guangxi University, Nanning, 530004, China.
E-mail addresses: sdyczm@gxu.edu.cn (M. Zhang), kefuyu@scsio.ac.cn (K. Yu).
[1] These authors contributed equally to this work.

https://doi.org/10.1016/j.bios.2023.115790
Received 28 September 2023; Accepted 24 October 2023
Available online 28 October 2023

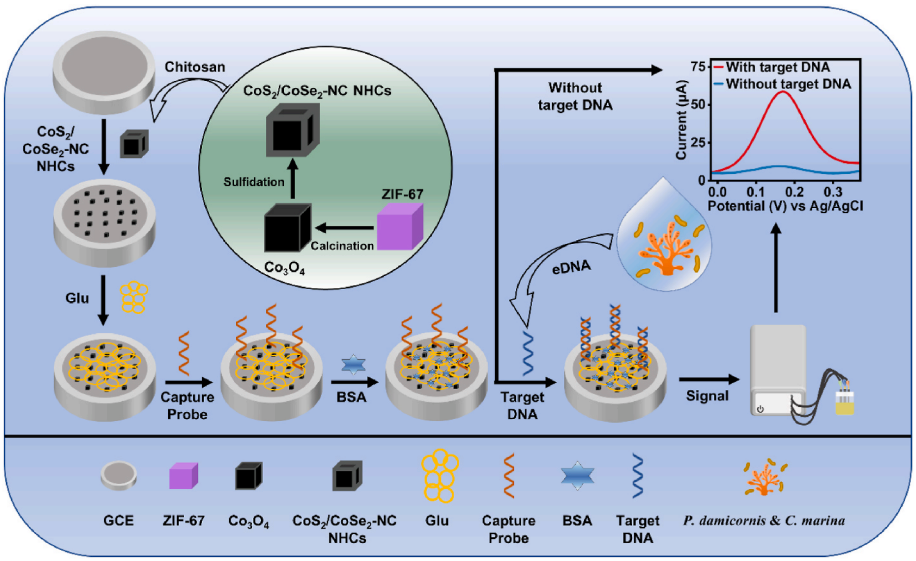

Fig. 1. The construction of an electrochemical biosensor.

ecological surveys (Takahashi et al., 2023). Lee et al. utilized eDNA approaches to detect bacterial communities' diversity and spatiotemporal dynamics in sediments and assess the corresponding correlation with environmental variables (Lee et al., 2020). In addition, eDNA techniques have been employed in the diversity research of marine fishes (Valdivia-Carrillo et al., 2021) and in monitoring the density of crown-of-thorns starfish (Uthicke et al., 2022; L. Wang et al., 2023). However, eDNA is vulnerable to various abiotic and biotic factors, such as temperature, water matrix, etc., and thus is difficult to store and transport for long periods (McCartin et al., 2022). Therefore, it is necessary to develop a rapid and on-site eDNA detection method.

Electrochemical biosensors have emerged as an ideal platform for

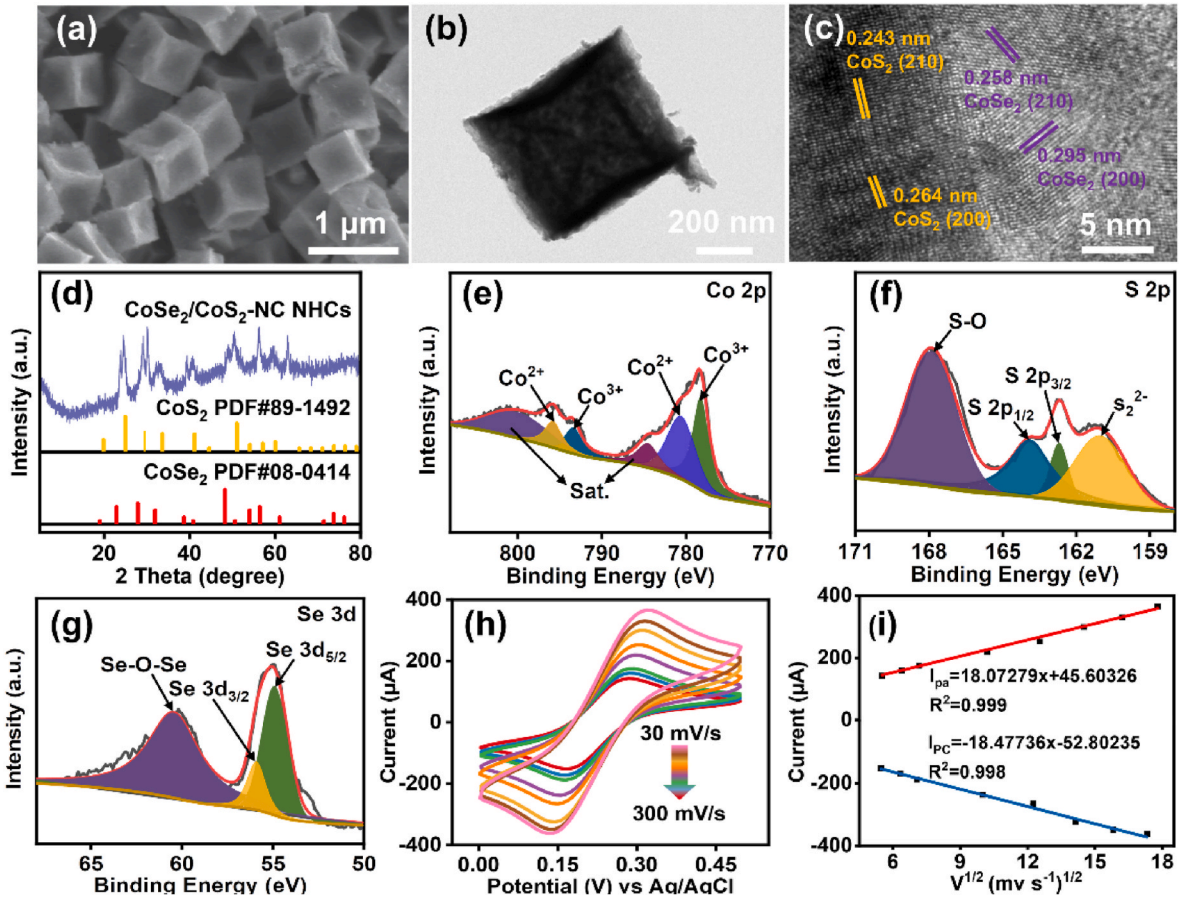

Fig. 2. (a–d) SEM, TEM, HRTEM elemental images and XRD patterns of CoS_2/$CoSe_2$-NC HNCs; XPS spectra of (e) Co 2p, (f) S 2p, (g) Se 3d; (h) CV curves of CoS_2/$CoSe_2$-NC HNCs at different scan rates; (i) the linear relationship of CoS_2/$CoSe_2$-NC HNCs between redox peak current and square root values of the scan rates. The error bars represented the standard error of the mean.

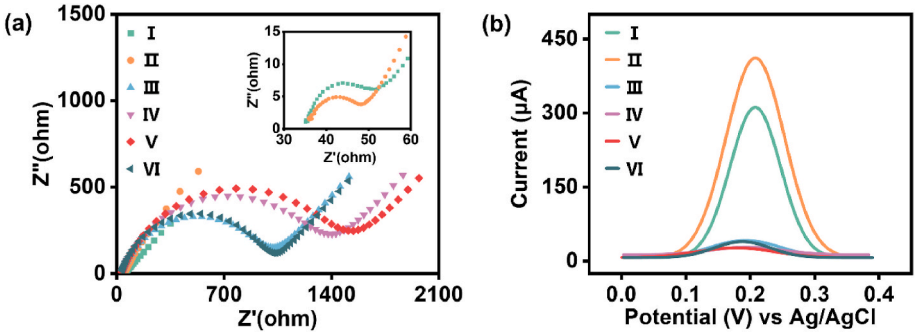

Fig. 3. (a) Nyquist plots of the EIS measurements and (b) DPV curves of the different steps of biosensor analysis: (I) GCE, (II) $CoS_2/CoSe_2$-NC NHCs/GCE, (III) Glu/$CoS_2/CoSe_2$-NC NHCs/GCE, (IV) capture probe/Glu/$CoS_2/CoSe_2$-NC NHCs/GCE, (V) BSA/capture probe/Glu/$CoS_2/CoSe_2$-NC NHCs/GCE, (VI) target DNA/BSA/capture probe/Glu/$CoS_2/CoSe_2$-NC NHCs/GCE. All experiments were performed in 0.1 M KCl/5.0 mM $[Fe(CN)_6]^{3-/4-}$.

effectively monitoring eDNA based on the Watson-Crick pairing principle. Compared with traditional detection methods, electrochemical biosensors have significant advantages in detecting probiotics due to their portability characteristics, high sensitivity, and operation convenience (Feng et al., 2020). Notably, a variety of electrochemical biosensors have been widely used in the investigation of food pathogens (Li et al., 2021; Riu and Giussani, 2020; Wasiewska et al., 2023) and marine pathogens (W. Wang et al., 2023; Wei et al., 2021). However, to our knowledge, few studies have reported on detecting *C. marina* eDNA using electrochemical biosensors. Hence, constructing a highly selective electrochemical biosensor for the effective on-site detection of *C. marina* eDNA would be of great significance.

In this study, we developed electrochemical biosensors with a lower limit of detection (LOD) and wider detection range by immobilizing specific oligonucleotide probes on the surface of the $CoS_2/CoSe_2$-NC heterojunction nanocubes ($CoS_2/CoSe_2$-NC HNCs) electrode material. The electrochemical biosensors were used for the rapid and accurate on-site detection of *C. marina* eDNA. Furthermore, the reliability and accuracy of the biosensors were verified by comparing them with the gold standard method of ddPCR. In addition, a mapping relationship was constructed between electrochemical biosensor detection results, coral probiotic concentration and coral health status. This study will provide new insights into the on-site inspection of probiotics and assessing the environmental tolerance of corals.

2. Materials and methods

The experimental details including Chemicals and Apparatus (**S1.1**–**1.2**), Synthesis of $CoS_2/CoSe_2$-NC HNCs (**S1.3**), Bacterial culture and DNA extraction (**S1.4**), Primers and probes design (**S1.5**), and Electrochemical measurement (**S1.6**) can be found in the Supporting **Information**.

2.1. Fabrication of electrochemical biosensors

All the probe sequences were shown in Table S1. The bare glassy carbon electrode (GCE) was initially polished to a mirror state with 1, 0.3, and 0.05 μm alumina powder, respectively, and sonicated with ethanol and deionized water for 5 min. Then, 10 μL of $CoS_2/CoSe_2$-NC HNCs solution (4 mg/mL) diluted with 1% chitosan was immobilized on the surface of the cleaned GCE. After immobilization, 10 μL of 2.5% glutaraldehyde (Glu) solution was added dropwise to the surface of the modified electrode, which was noted as Glu/$CoS_2/CoSe_2$-NC HNCs/GCE. Then, 10 μL of 0.5 μM capture probe was added dropwise onto Glu/$CoS_2/CoSe_2$-NC HNCs/GCE. The modified electrode was then added onto 10 μL bovine serum albumin buffer (BSA, 0.1%, v/v) to block the non-specific binding sites, which was noted as BSA/capture probe/Glu/$CoS_2/CoSe_2$-NC HNCs/GCE. Finally, the electrode was incubated with 10 μL of different concentrations of target DNA and incubated at room temperature for 1 h, followed by phosphate buffer solution (PBS) washing before the electrochemical performance was measured. Finally, the constructed electrodes were stored at 4 °C. The preparation process of the biosensor was presented graphically in Fig. 1.

2.2. Coral material and probiotic-heat stress experiment

Three treatments were established: control (26 °C), HSCM (30 °C of heat stress and inoculated with 1 mL 10^7 CFU/mL of *C. marina*), and HS (30 °C of heat stress). The corresponding experimental details can be found in Supporting **Information**, **S1.7**–**1.10**.

3. Results and discussion

3.1. Characterization of the $CoS_2/CoSe_2$-NC HNCs

The morphology of the $CoS_2/CoSe_2$-NC HNCs was characterized by scanning electronic microscopy (SEM) (Fig. 2a) and transmission electron microscopy (TEM) Fig. 2b), which indicated that the $CoS_2/CoSe_2$-NC HNCs retained the cubic structure of the template ZIF-67 with a size of ~500 nm. Furthermore, the energy dispersive spectroscopy (EDS) maps (Fig. S1) confirmed the presence of Co, S, Se, C, and N elements uniformly distributed over the $CoS_2/CoSe_2$-NC HNCs. High-resolution TEM image (Fig. 2c) revealed the three sets of lattice fringe spacings of 0.243 nm and 0.264 nm for the (210) and (200) plane of CoS_2, 0.258 and 0.295 nm for (210) and (200) planes of $CoSe_2$, respectively. XRD pattern shown in Fig. 2d proved that the diffraction peaks of $CoS_2/CoSe_2$-NC HNCs were consistent with those of CoS_2 (JCPDS 89-1492) and $CoSe_2$ (JCPDS 08-0413), which indicated the successful preparation of the electrode material $CoS_2/CoSe_2$-NC HNCs. Noteworthy, the diffraction peaks of the $CoS_2/CoSe_2$-NC HNCs were slightly right-shifted, which might be attributed to the doping of Se and S elements, leading to lattice distortion and defects in the $CoS_2/CoSe_2$-NC HNCs. The surface composition and chemical state of the $CoS_2/CoSe_2$-NC HNCs were investigated by X-ray photoelectron spectroscopy (XPS). The survey-scan spectrum (Fig. 2e–g, Fig. S2) displayed the existence of Co, S, Se, C, and N signals in the $CoS_2/CoSe_2$-NC HNCs, consistent with EDX element analysis. All the above analyses confirmed the successful preparation of the $CoS_2/CoSe_2$-NC HNCs. The presence of a large number of heterogeneous interfaces caused a large number of lattice defects and distortions that could adjust the electronic structure and enhance the interfacial charge transfer (Li et al., 2022). Therefore, the $CoS_2/CoSe_2$-NC HNCs had good electrocatalytic properties and could significantly amplify the electrical signal of the biosensor.

The electroactive surface area of the electrode material is extremely important in the electrochemical properties (Sun et al., 2022). Therefore, the electroactive surface area of $CoS_2/CoSe_2$-NC HNCs electrodes was calculated by CV (Fig. 2h) at different scan rates from 30 to 300 mV/s, where the square root of the scan rate increased with increasing

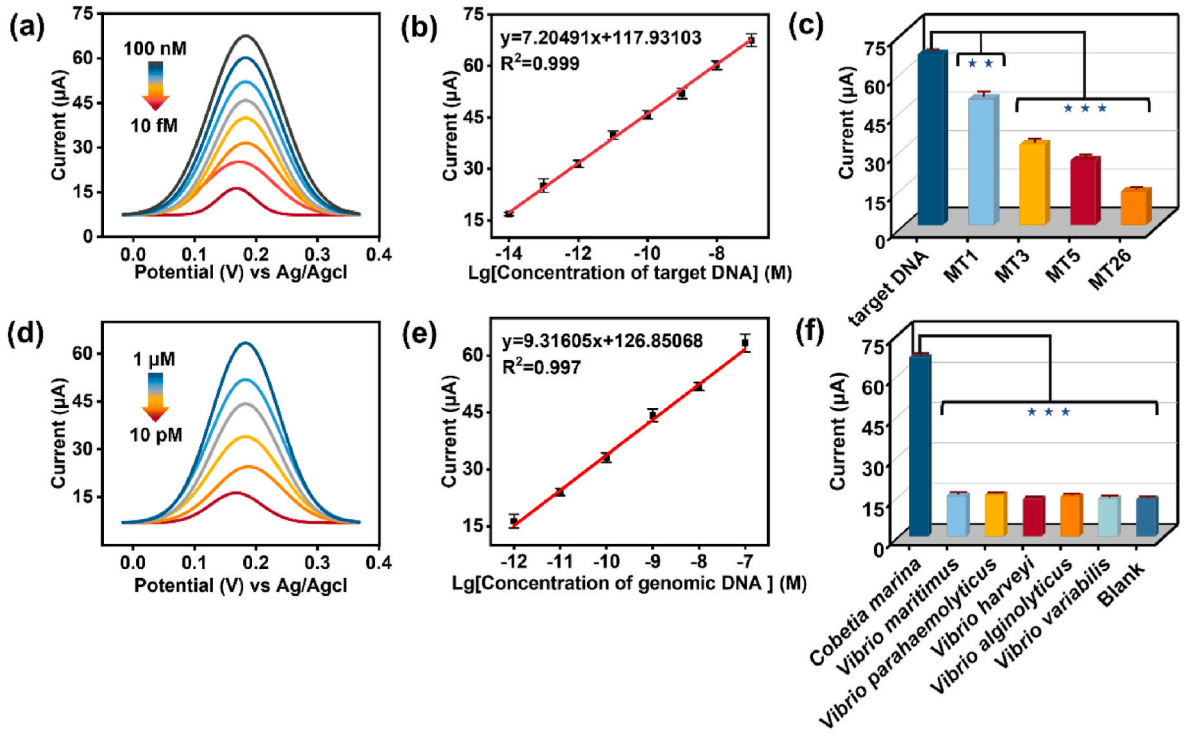

Fig. 4. (a) DPV curves for the detection of synthetic target DNA at different concentrations, (b) corresponding linear trend of the peak current versus the logarithm of the concentration of synthetic target DNA, (c) specificity of the biosensor hybridized to different 10 nM mismatched DNA sequences (RSD = 1.86%, 3.89%, 4.66%, 5.62%, and 6.38%), (d) DPV curves for the detection of *C. marina* genomic DNA at different concentrations, (e) corresponding linear trend of the peak current versus the logarithm of the concentration of *C. marina* genomic DNA, (f) specificity of the biosensor based on the *C. marina* genome versus various interfering genomes (RSD = 1.48%, 5.32%, 2.54%, 2.37%, 3.91%, 4.36% and 4.02%). The error bars represented the standard error of the mean. **: $0.001 < P < 0.01$, ***: $P < 0.001$.

oxidation peak current (Fig. 2i). The electroactive surface area of $CoS_2/CoSe_2$-NC HNCs electrodes was 0.186 cm^2 calculated from the Randes - Sevcik equation (**S1.11**, Supporting **Information**) (L. Wang et al., 2023). Based on all the above discussions, $CoS_2/CoSe_2$-NC HNC electrodes can promote the charge transfer rate and provide an excellent conductive platform for the prepared electrochemical biosensor.

3.2. Construction of the electrochemical biosensor

In the Nyquist plots of the EIS measurements, the diameter of the semicircle is positively correlated with the resistance value. Thus, the EIS measurements were performed for the electrochemical biosensor at different stages of construction. As shown in Fig. 3a, after $CoS_2/CoSe_2$-NC HNCs immobilizing onto the GCE, a smaller charge transfer resistance was observed, and the impedance of $CoS_2/CoSe_2$-NC HNCs/GCE was only 10 Ω. On that basis, Glu/$CoS_2/CoSe_2$-NC HNCs/GCE was formed by adding the binder Glu, and the impedance value increased dramatically. Subsequently, the capture probe was immobilized on the modified electrode surface due to the sulfhydryl group introduced at the end of the proposed capture probe can undergo a thiol-aldehyde addition (TAA) reaction with the glutaraldehyde aldehyde group (Yang et al., 2021; Zhang et al., 2021), denoted as capture probe/Glu/$CoS_2/CoSe_2$-NC HNCs/GCE. Since the increased density of negative charges and the resulting increase in electrostatic repulsion of $[Fe(CN)_6]^{3-/4-}$ anions (Ji et al., 2022), the impedance value increased again at this stage. After the BSA solution was assembled onto the modified electrode blocking the non-specific binding sites, the electrochemical signal response slightly increased, because the non-conductive substances of BSA could hinder the electron transfer. Lastly, when target DNA was introduced, it hybridized with a capture probe to form a double-stranded DNA according to the Watson-Crick base pairing principle. As the phosphate backbone of the double-stranded DNA served as an efficient charge conduction line (Zhuravel et al., 2020), facilitating electron transfer between the sensing interface and the solution, the impedance value was subsequently reduced. Correspondingly, different construction stages of the electrochemical biosensor were further characterized by the DPV (Fig. 3b); the outcomes of DPV curves correspond well to the EIS results, indicating the successful construction of the electrochemical biosensor.

The testing conditions were optimized to achieve this sensing platform's optimal performance. As shown in Fig. S3, the optimal detection parameters were set as capture probe concentration of 0.5 μM (10 μL), target DNA incubation time of 1 h, pH 7.4, with the $CoS_2/CoSe_2$-NC HNCs concentration of 4 mg/mL (10 μL). Subsequent experiments for electrochemical performance characterization were performed using the optimized parameters.

3.3. Performance of electrochemical biosensors

The proposed electrochemical sensing system was exploited to detect target DNA under optimal experimental conditions. From Fig. 4a, it was noted that the DPV responses enhanced with increasing the concentration of target DNA ranged from 10 fM to 100 nM due to DNA hybridization, thus reducing the steric hindrance of the surface and promoting interfacial electron transfer. Meanwhile, Fig. 4b showed an excellent linear relationship between the peak current and the logarithmic value of target DNA concentration, and the linear relationship was shown in Equation (1):

$$y = 7.20491x + 117.93103\ ,\ R^2 = 0.999 \quad (1)$$

LOD (**S1.12**, Supporting **Information**) (Zhang et al., 2023) for target DNA was calculated to be as low as 1.58 fM. Compared to similar electrochemical biosensors for bacteria detection (Table S2), the developed biosensor had a wide linear range and a low LOD, indicating the excellent potential of this biosensor for on-site monitoring of *C. marina* eDNA.

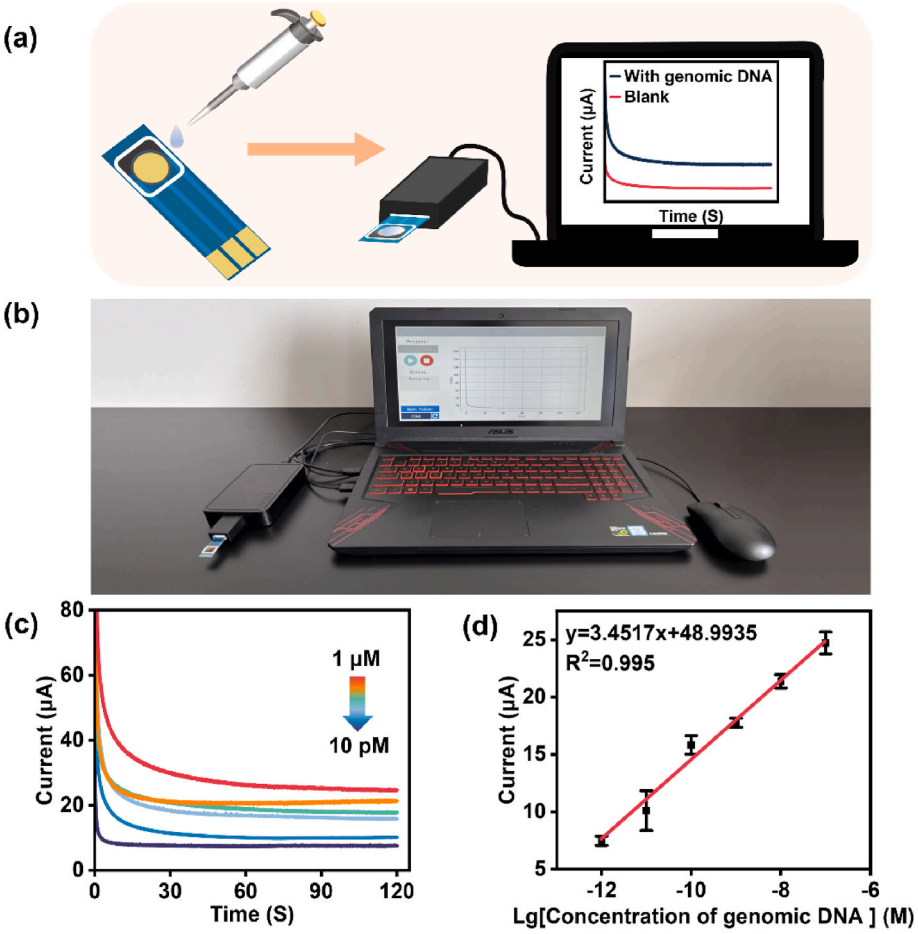

Fig. 5. (a) Schematic diagram of the portable device, (b) photo of a portable device at work, (c) i-t curves for the detection of *C. marina* genomic DNA at different concentrations, and (d) linear relationship between the current and the logarithm of the amount of *C. marina* genomic DNA. The error bars represented the standard error of the mean.

The specificity of the DNA probe is crucial for the biosensor. Thus, the mismatched DNA sequences had to be distinguished by different electrochemical biosensor responses. The target sequence mutations at different locations were artificially designed (Table S1). As shown in Fig. 4c, the current was the highest when the complementary sequence probe completely hybridized the biosensor. This indicates that the two sequences were bound effectively on the electrode surface and boosted charge transfer. Moreover, compared with the complementary target DNA, the one-base (MT1), three-base (MT3), five-base (MT5), and non-complementary (MT26) mismatched DNA sequences were reduced by 26.17%, 52.95%, 62.18%, and 80.13%, respectively, with significant differences ($P < 0.05$).

In addition, we further verified the electrochemical biosensor detection of different concentrations of *C. marina* genomic DNA (10 pM–1 μM). As shown in Fig. 4d, a gradual increase in current was observed as the *C. marina* genomic DNA concentration increased. The change of current was linearly related to the logarithms of the concentration of *C. marina* genomic DNA (Fig. 4e), as shown in Equation (2):

$$y = 9.31605x + 126.85068\ ,\ R^2 = 0.997 \quad (2)$$

Correspondingly, the calculated LOD for *C. marina* genomic DNA was 6.5 pM, demonstrating that the proposed biosensor provided an effective mean for *C. marina* eDNA on-site detection.

In this study, the specificity of the biosensor was investigated with five marine bacterial strains, including *Vibrio maritimus*, *Vibrio parahaemolyticus*, *Vibrio harveyi*, *Vibrio alginolyticus, Vibrio variabilis,* and blank sample. The DNA concentration of *C. marina* was 100 nM; the other strains DNA concentration was 1 μM, and the blank sample without any species DNA. As shown in Fig. 4f, the current value of the *C. marina* DNA sample was approximately 6 times greater than the other strains DNA samples and the blank sample, while the current values of the other strains DNA samples were close to the blank sample. Furthermore, the findings demonstrated a noteworthy distinction between the *C. marina* DNA sample and other DNA samples, consistent with the results of the primer specificity analysis (Fig. S4). The above results illustrated that the biosensor has excellent specificity and immunity to interference.

3.4. Repeatability and stability of electrochemical biosensor

To verify the repeatability, five different GCE electrodes were used to detect the same concentration (1 nM) of target DNA (Fig. S5a), and each electrode was tested three times. The results showed little difference ($P > 0.05$). The corresponding relative standard deviation (RSD) was 1.47%, demonstrating the designed biosensor's excellent repeatability (**S1.13**, Supporting **Information**).

Furthermore, the stability of the fabricated biosensor was crucial for practical applications, especially in complex field environments. Thus, the stability was estimated and monitored every two days. As displayed in Fig. S5b, the currents did not fluctuate significantly ($P > 0.05$) when the proposed sensing platform was treated with 1 nM target DNA, and the RSD of 3.22% demonstrated that the proposed biosensor possessed good stability.

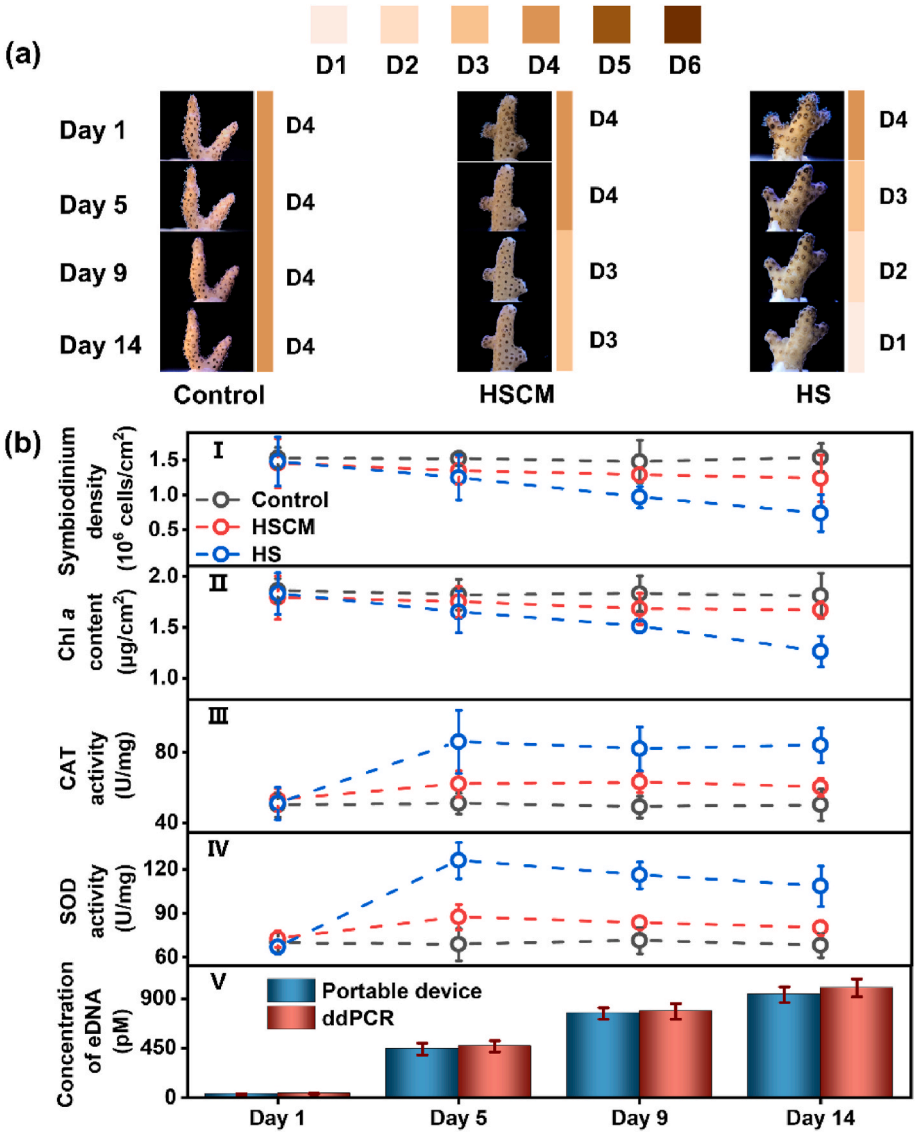

Fig. 6. Protection from thermal stress with coral probiotics *C. marina*. (a) Photos of coral nubbins under three treatments s on Day 1, 5, 9, and 14, (b) physiological and biochemical indices of *P. damicornis* and the detection of *C. marina* eDNA in HSCM treatments: (I) Symbiodiniaceae density, (II) Chl *a* content, (III) SOD activity and (IV) CAT activity of *P. damicornis*, and (V) the portable device and ddPCR for the detection of *C. marina* eDNA in HSCM treatments. The error bars represented the standard error of the mean.

3.5. Portable detection

The portable device assay process consists of eDNA extraction and electrochemical detection, which can be easily completed on site within 100 min. Therefore, a portable device was used for on-site detection with miniaturization and wireless data transmission advantages. Fig. 5a and b showed a schematic diagram of its detection process and a photo of portable electrochemical at work, which a non-specialized person could perform outside the laboratories with a laptop computer.

Fig. 5c showed the i-t curves with the *C. marina* genomic DNA concentration range from 10 pM to 1 μM, in which a gradual current decrease was observed as the genomic DNA concentration increased. Besides, there was a strong linear relationship between the current values and the logarithm of genomic DNA concentration in the investigated concentration range (Fig. 5d), and the regression equation was shown in Equation (3):

$$y = 3.4517x + 48.9935\ ,\ R^2 = 0.995 \quad (3)$$

The calculated LOD for *C. marina* genomic DNA was 7.4 pM. The wide linear response range and low LOD value of the proposed portable device confirmed the effectiveness in the application field. These results demonstrated the excellent reproducibility and stability of the designed portable device and proved that the portable device was capable of the on-site detection of C. marina eDNA with high accuracy even in complex field environments.

3.6. Assessment of probiotic effects by biosensors

The visual appearance of *Pocillopora damicornis* coral nubbins, assessed using the Coral Health Chart (Siebeck et al., 2006), demonstrated that all treatments maintained at 26 °C displayed no visible color pigment shift during the 14 days of the whole experiment. In contrast, all replicates of the HS treatment (heat stress) raised to 30 °C displayed clear signs of bleaching with a decrease of 3 units based on the Coral Health Chart; while for the HSCM treatment (with *C. marina* addition), all replicates also showed a 1-unit decrease from Day 9–14, although no visual shifts were detected (Fig. 6a). Meanwhile, Symbiodiniaceae density and Chl *a* content decreased significantly in HS treatment after

heat stress during 14 days ($P < 0.05$), but no significant differences could be observed in both control and HSCM treatment (Fig. 6b, Tables S3–4). Furthermore, direct exposure to 30 °C resulted in a significant increase in superoxide dismutase (SOD) and CAT activities compared with those in the control and HSCM treatment ($P < 0.05$) (Fig. 6b, Tables S5–6).

In addition, from Day 1–14, the electronic device detected the eDNA concentrations of *C. marina* in HSCM treatment (Fig. 6b) which significantly increased from Day 1–9. However, the increasing trend slowed down from Day 9 onwards. Specifically, the eDNA concentration increased from 32 to 441 pM during the initial five days without visible colour pigment shift in the HSCM treatment; eDNA concentration increased from 441 to 764 pM during Day 5–9 with decreases of 1 unit; finally, the increase in eDNA concentration from 764 to 935 pM showed no colour pigment shift and no signs of bleaching from Day 9–14. Then the accuracy of the biosensor was verified by comparison with the ddPCR method ($P > 0.05$) (Fig. 6b, Table S7). Besides, a comparison of the performance characteristics of the designed portable device and currently reported method in the detection of eDNA was presented in Table S8, which demonstrated the faster response and low-cost advantages of the proposed electrochemical sensing strategy. Experimental errors were eliminated by sample blanks, filter blanks, and washed vessel blanks analyses (**S1.14**, Fig. S6). Above all, the results showed that the biosensor was capable of reflecting the protective effect of probiotics on coral heat stress, and the proposed technique will put new insights in the rapid and on-site detection of coral probiotics to assist corals against global warming.

4. Conclusion

In this work, an efficient electrochemical biosensor was developed based on $CoS_2/CoSe_2$-NC HNCs electrode material with a specific DNA probe for the on-site detection of the coral probiotic, *C. marina*. After optimization, the electrochemical biosensor displayed excellent performance with a wide linear range of 10 fM to 100 nM and an LOD of 1.58 fM. Additionally, the portable device had been successfully constructed with a linear range from 10 pM to 1 μM, and the LOD of 7.4 pM. Furthermore, the accuracy and reliability of the biosensors were verified by ddPCR ($P > 0.05$), and the average cost for each analysis was only ~ $1.08 while the whole analysis procedure was within 100 min with reliable sensitivity and specificity. The eDNA concentration detected by the electrochemical biosensor correlated well with the effectiveness of the probiotic in protecting corals from heat stress, thus suggesting that the biosensors could be utilized as an ideal evaluation tool for the efficiency of coral probiotics.

CRediT authorship contribution statement

Liwei Wang: Conceptualization; Performed literature search, Data curation, Investigation, Methodology, and Writing original draft. Qi Bin: Experimentation, Writing-review & editing, Conceptualization, Data curation. Hongjie Liu: Writing – review & editing. Yibo Zhang: Investigation, Data curation. Shaopeng Wang: Performed literature search, Data curation. Songlin Luo: Software, Validation. Zhenghua Chen: Software, Validation. Man Zhang: Manuscript editing. Kefu Yu: Manuscript editing.

Declaration of competing interest

The authors declare that they have no known competing financial interests or personal relationships that could have appeared to influence the work reported in this paper.

Data availability

Data will be made available on request.

Acknowledgments

This work was funded by the National Natural Science Foundation of China (42030502, 42090041), Key Projects of Guangxi Natural Science Foundation (No. 2020GXNSFDA297015), China; Natural Science Foundation of Guangxi Province (No. 2022GXNSFAA035565), China.

Appendix A. Supplementary data

Supplementary data to this article can be found online at https://doi.org/10.1016/j.bios.2023.115790.

References

Buerger, P., Alvarez-Roa, C., Coppin, C.W., Pearce, S.L., Chakravarti, L.J., Oakeshott, J. G., Edwards, O.R., van Oppen, M.J.H., 2020. Heat-evolved microalgal symbionts increase coral bleaching tolerance. Sci. Adv. 6, 1–9. https://doi.org/10.1126/sciadv.aba2489.

Feng, Y., Zhou, D., Gao, L., He, F., 2020. Electrochemical biosensor for rapid detection of bacteria based on facile synthesis of silver wire across electrodes. Biosens. Bioelectron. 168, 112527 https://doi.org/10.1016/j.bios.2020.112527.

Huang, S., Yoshitake, K., Watabe, S., Asakawa, S., 2022. Environmental DNA study on aquatic ecosystem monitoring and management: recent advances and prospects. J. Environ. Manag. 323, 116310 https://doi.org/10.1016/j.jenvman.2022.116310.

Ji, Y., Guo, J., Ye, B., Peng, G., Zhang, C., Zou, L., 2022. An ultrasensitive carcinoembryonic antigen electrochemical aptasensor based on 3D DNA nanoprobe and Exo III. Biosens. Bioelectron. 196, 113741 https://doi.org/10.1016/j.bios.2021.113741.

Lee, A.H., Lee, J., Hong, S., Kwon, B.O., Xie, Y., Giesy, J.P., Zhang, X., Khim, J.S., 2020. Integrated assessment of west coast of South Korea by use of benthic bacterial community structure as determined by eDNA, concentrations of contaminants, and in vitro bioassays. Environ. Int. 137, 105569 https://doi.org/10.1016/j.envint.2020.105569.

Li, F., Ye, Q., Chen, M., Zhou, B., Zhang, J., Pang, R., Xue, L., Wang, J., Zeng, H., Wu, S., Zhang, Y., Ding, Y., Wu, Q., 2021. An ultrasensitive CRISPR/Cas12a based electrochemical biosensor for Listeria monocytogenes detection. Biosens. Bioelectron. 179, 113073 https://doi.org/10.1016/j.bios.2021.113073.

Li, W., Wu, L., Wu, X., Shi, C., Li, Y., Zhang, L., Mi, H., Zhang, Q., He, C., Ren, X., 2022. Regulation and mechanism study of the CoS2/Cu2S-NF heterojunction as highly-efficient bifunctional electrocatalyst for oxygen reactions. Appl. Catal., B 303. https://doi.org/10.1016/j.apcatb.2021.120849.

Liu, X., Xiao, P., Guo, Y., Liu, L., Yang, J., 2019. The impacts of different high-throughput profiling approaches on the understanding of bacterial antibiotic resistance genes in a freshwater reservoir. Sci. Total Environ. 693, 133585 https://doi.org/10.1016/j.scitotenv.2019.133585.

Liu, Y., Liu, B., Li, D., Hu, Y., Zhao, L., Zhang, M., Ge, S., Pang, J., Li, Yixuan, Wang, R., Wang, P., Huang, Y., Huang, J., Bai, J., Ren, F., Li, Yuan, 2020. Improved gastric acid resistance and adhesive colonization of probiotics by mucoadhesive and intestinal targeted konjac glucomannan microspheres. Adv. Funct. Mater. 30 https://doi.org/10.1002/adfm.202001157.

Maire, J., van Oppen, M.J.H., 2022. A role for bacterial experimental evolution in coral bleaching mitigation? Trends Microbiol. 30, 217–228. https://doi.org/10.1016/j.tim.2021.07.006.

Mauvisseau, Q., Harper, L.R., Sander, M., Hanner, R.H., Kleyer, H., Deiner, K., 2022. The multiple states of environmental DNA and what is known about their persistence in aquatic environments. Environ. Sci. Technol. 56, 5322–5333. https://doi.org/10.1021/acs.est.1c07638.

McCartin, L.J., Vohsen, S.A., Ambrose, S.W., Layden, M., McFadden, C.S., Cordes, E.E., McDermott, J.M., Herrera, S., 2022. Temperature controls eDNA persistence across physicochemical conditions in seawater. Environ. Sci. Technol. 56, 8629–8639. https://doi.org/10.1021/acs.est.2c01672.

Quigley, K.M., Ramsby, B., Laffy, P., Harris, J., Mocellin, V.J.L., Bay, L.K., 2022. Symbioses are restructured by repeated mass coral bleaching. Sci. Adv. 8, 1–13. https://doi.org/10.1126/sciadv.abq8349.

Riu, J., Giussani, B., 2020. Electrochemical biosensors for the detection of pathogenic bacteria in food. TrAC, Trends Anal. Chem. 126, 115863 https://doi.org/10.1016/j.trac.2020.115863.

Rosado, P.M., Leite, D.C.A., Duarte, G.A.S., Chaloub, R.M., Jospin, G., Nunes da Rocha, U., Saraiva, J, P., Dini-Andreote, F., Eisen, J.A., Bourne, D.G., Peixoto, R.S., 2019. Marine probiotics: increasing coral resistance to bleaching through microbiome manipulation. ISME J. 13, 921–936. https://doi.org/10.1038/s41396-018-0323-6.

Siebeck, U.E., Marshall, N.J., Klüter, A., Hoegh-Guldberg, O., 2006. Monitoring coral bleaching using a colour reference card. Coral Reefs 25, 453–460. https://doi.org/10.1007/s00338-006-0123-8.

Silva, D.P., Villela, H.D.M., Santos, H.F., Duarte, G.A.S., Ribeiro, J.R., Ghizelini, A.M., Vilela, C.L.S., Rosado, P.M., Fazolato, C.S., Santoro, E.P., Carmo, F.L., Ximenes, D.S., Soriano, A.U., Rachid, C.T.C.C., Vega Thurber, R.L., Peixoto, R.S., 2021. Multi-domain probiotic consortium as an alternative to chemical remediation of oil spills at coral reefs and adjacent sites. Microbiome 9, 1–19. https://doi.org/10.1186/s40168-021-01041-w.

Sun, X., Duan, M., Li, R., Meng, Y., Bai, Q., Wang, L., Liu, M., Yang, Z., Zhu, Z., Sui, N., 2022. Ultrathin graphdiyne/graphene heterostructure as a robust electrochemical sensing platform. Anal. Chem. 94, 13598–13606. https://doi.org/10.1021/acs.analchem.2c03387.

Takahashi, M., Saccò, M., Kestel, J.H., Nester, G., Campbell, M.A., van der Heyde, M., Heydenrych, M.J., Juszkiewicz, D.J., Nevill, P., Dawkins, K.L., Bessey, C., Fernandes, K., Miller, H., Power, M., Mousavi-Derazmahalleh, M., Newton, J.P., White, N.E., Richards, Z.T., Allentoft, M.E., 2023. Aquatic environmental DNA: a review of the macro-organismal biomonitoring revolution. Sci. Total Environ. 873 https://doi.org/10.1016/j.scitotenv.2023.162322.

Tandon, K., Lu, C.Y., Chiang, P.W., Wada, N., Yang, S.H., Chan, Y.F., Chen, P.Y., Chang, H.Y., Chiou, Y.J., Chou, M.S., Chen, W.M., Tang, S.L., 2020. Comparative genomics: dominant coral-bacterium Endozoicomonas acroporae metabolizes dimethylsulfoniopropionate (DMSP). ISME J. 14, 1290–1303. https://doi.org/10.1038/s41396-020-0610-x.

Thatcher, C., Høj, L., Bourne, D.G., 2022. Probiotics for coral aquaculture: challenges and considerations. Curr. Opin. Biotechnol. 73, 380–386. https://doi.org/10.1016/j.copbio.2021.09.009.

Ushijima, B., Gunasekera, S.P., Meyer, J.L., Tittl, J., Pitts, K.A., Thompson, S., Sneed, J. M., Ding, Y., Chen, M., Jay Houk, L., Aeby, G.S., Häse, C.C., Paul, V.J., 2023. Chemical and genomic characterization of a potential probiotic treatment for stony coral tissue loss disease. Commun. Biol. 6, 248. https://doi.org/10.1038/s42003-023-04590-y.

Uthicke, S., Robson, B., Doyle, J.R., Logan, M., Pratchett, M.S., Lamare, M., 2022. Developing an effective marine eDNA monitoring: eDNA detection at pre-outbreak densities of corallivorous seastar (Acanthaster cf. solaris). Sci. Total Environ. 851, 158143 https://doi.org/10.1016/j.scitotenv.2022.158143.

Valdivia-Carrillo, T., Rocha-Olivares, A., Reyes-Bonilla, H., Domínguez-Contreras, J.F., Munguia-Vega, A., 2021. Integrating eDNA metabarcoding and simultaneous underwater visual surveys to describe complex fish communities in a marine biodiversity hotspot. Mol. Ecol. Resour. 21, 1558–1574. https://doi.org/10.1111/1755-0998.13375.

Wang, L., Xu, J., Liu, H., Wang, S., Ou, W., Zhang, M., Wei, F., Luo, S., Chen, B., Zhang, S., Yu, K., 2023. Ultrasensitive and on-site eDNA detection for the monitoring of crown-of-thorns starfish densities at the pre-outbreak stage using an electrochemical biosensor. Biosens. Bioelectron. 230, 115265 https://doi.org/10.1016/j.bios.2023.115265.

Wang, W., Xiao, S., Zeng, M., Xie, H., Gan, N., 2023. Dual-mode colorimetric-electrochemical biosensor for Vibrio parahaemolyticus detection based on CuO2 nanodot-encapsulated metal-organic framework nanozymes. Sensor. Actuator. B Chem. 387, 133835 https://doi.org/10.1016/j.snb.2023.133835.

Wasiewska, L.A., Juska, V.B., Seymour, I., Burgess, C.M., Duffy, G., O'Riordan, A., 2023. Electrochemical nucleic acid-based sensors for detection of Escherichia coli and Shiga toxin-producing E. coli —review of the recent developments. Compr. Rev. Food Sci. Food Saf. 1–25. https://doi.org/10.1111/1541-4337.13132.

Wei, W., Lin, H., Hao, T., Wang, S., Hu, Y., Guo, Z., Luo, X., 2021. DNA walker-mediated biosensor for target-triggered triple-mode detection of Vibrio parahaemolyticus. Biosens. Bioelectron. 186, 113305 https://doi.org/10.1016/j.bios.2021.113305.

Xia, L.Y., Tang, Y.N., Zhang, J., Dong, T.Y., Zhou, R.X., 2022. Advances in the DNA nanotechnology for the cancer biomarkers analysis: attributes and applications. Semin. Cancer Biol. 86, 1105–1119. https://doi.org/10.1016/j.semcancer.2021.12.012.

Yang, R., Liu, X., Ren, Y., Xue, W., Liu, S., Wang, P., Zhao, M., Xu, H., Chi, B., 2021. Injectable adaptive self-healing hyaluronic acid/poly (γ-glutamic acid) hydrogel for cutaneous wound healing. Acta Biomater. 127, 102–115. https://doi.org/10.1016/j.actbio.2021.03.057.

Zhang, J., Hurren, C., Lu, Z., Wang, D., 2023. Nanofiber-based colorimetric platform for point-of-care detection of E. coli. Chem. Eng. J. 463, 142357 https://doi.org/10.1016/j.cej.2023.142357.

Zhang, Y., Li, X., Bai, G., Wei, W., Liu, X., 2021. Hyperbranched polymer with dynamic thiol-aldehyde crosslinking and its application as a self-healable bioadhesive. J. Mater. Chem. B 9, 5818–5828. https://doi.org/10.1039/d1tb00929j.

Zhuravel, R., Huang, H., Polycarpou, G., Polydorides, S., Motamarri, P., Katrivas, L., Rotem, D., Sperling, J., Zotti, L.A., Kotlyar, A.B., Cuevas, J.C., Gavini, V., Skourtis, S. S., Porath, D., 2020. Backbone charge transport in double-stranded DNA. Nat. Nanotechnol. 15, 836–840. https://doi.org/10.1038/s41565-020-0741-2.